2024 IEEE/RSJ International Conference on Intelligent Robots and Systems (IROS)
October 14-18, 2024. Abu Dhabi, UAE

# Design, Prototype, and Performance Assessment of an Autonomous Manipulation System for Mars Sample Recovery Helicopter

Arash Kalantari, Alex Brinkman, Kalind Carpenter, Matthew Gildner, Justin Jenkins,
David Newill-Smith, Jeffrey Seiden, Allen Umali, Ryan Mccormick

***Abstract*— This paper presents the design, prototype, and testing of a 150 g (current best estimate) manipulation system that enables Mars Sample Recovery Helicopter (SRH) concept to autonomously pickup, stow, and drop-off Returnable Sample Tube and Glove Assemblies (RGAs) on the surface of Mars next to the Sample Retrieval Lander (SRL). It consists of a 3 DOF planar Robotic Arm (RA), a novel 2 DOF Gripper with compliant fingers, and a Stow Mechanism. Within the planned Mars Sample Return (MSR) campaign, two SRHs would operate in parallel to retrieve and transfer total of 10 RGAs (146g each) to the SRL, as the backup to the Perseverance Rover. Once SRH arrives at the target pickup location, the RA places the Gripper precisely over the RGA. The gripper grabs and picks up RGAs using a linkage based non-back-drivable mechanism and its compliant fingers. Subsequently, the RA is secured into the stow features, following dislodging rocks and pebbles, by going through a specific sequence of joint trajectories. This ensures the RA and RGA are stable and secure during transit to the SRL while all Manipulation System actuators are powered off. The whole sequence of manipulation is performed autonomously using feedback of a pair of stereo-cameras and absolute encoders. Experimental evaluation of the Manipulation System performance has proved its robustness and consistency in successful RGA pickup, stow, and drop-off.**

## I. Introduction

The Mars Sample Recovery Helicopter (SRH) concept consists of a hybrid aerial and terrestrial mobility platform and a specialized light weight (150g, current best estimate) 5 degree of freedom (DOF) manipulation system (Figure 1). Within the planned Mars Sample Return (MSR) campaign, SRH's purpose is to be the secondary method of retrieval of the Returnable Sample Tube and Glove Assemblies (RGA) from the Martian surface. In the current concept of operation, two identical SRHs would operate in parallel, each taking off from SRL and using its in-flight map-based navigation system to reach and land at a predetermined helipad at a safe distance to RGA. Next, it would drive on the surface using visual-inertial navigation and visual-servoing to precisely position manipulation system in the vicinity of the RGA. Manipulation system is then responsible to reach down to the surface, acquire the RGA, and secure it on-board of the SRH for flight and drive back to the SRL. This paper presents design and development of the SRH manipulation system in detail.

The current MSR plan is to primarily use the Perseverance rover to carry RGAs directly to the SRL. However, should the rover become unable to deliver its onboard samples, the SRH concept is designed to collect 10 alternate RGA's previously left on the surface by Perseverance (Figure 3) and transport them to the SRL. This would help ensure the best chance of successfully returning a scientifically compelling selection of Mars rock and soil samples to Earth. SRH concept was initially proposed for MSR mission in 2022 [1]. It expands on Ingenuity's aerial mobility design, adding ground mobility and manipulation system. By adopting the Ingenuity's aerial mobility design, the SRH concept had constraints of relatively low mass and volume growth for new subsystem accommodation. These constraints lead to a challenging design problem for Ground Mobility and Manipulation Systems.

Authors are with the Jet Propulsion Laboratory, California Institute of Technology, 4800 Oak Grove Drive, Pasadena CA 91109 (e-mail: arash.kalantari@jpl.nasa.gov).

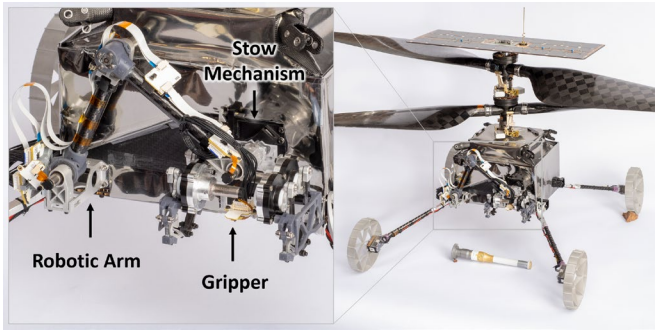


**Figure 1. SRH concept prototype consisting of Aerial Mobility, Ground Mobility, and Manipulation System**

The use of a fetch rover has been previously considered for MSR mission [2]. However, the traditional rover-based approach is challenged by uncertainties in landing zone, requiring the rover to travel long distances to reach the target site. This presents logistical complexities due to the requirement for large rovers, leading to high costs and technical challenges in spacecraft launch and deployment that can carry combined SRL and rover mass. Incorporating a flying platform would enable efficient long-distance travel with a compact vehicle, optimizing resource utilization and mission feasibility. Additionally, the integration of ground mobility enhances precision by facilitating direct navigation to target spots, following a close-proximity landing.

Rotorcrafts' ability to navigate diverse terrains, access hard-to-reach areas, and perform tasks such as aerial reconnaissance and transportation has made them a popular mobility platform. Many innovative concepts have been explored to enable rotorcrafts hybrid aerial and ground mobility for earth application [3] [4], where mass and volume has been much less constrained than SRH. Similar challenges are present for development of the manipulation system.

The addition of robotic arm and end effector to rotorcrafts further expands their applications by enabling them to physically interact with the environment and has led to their widespread adoption in various applications in both academic

and commercial domains including object transport and delivery [5], tool operation [6], wall climbing [7], and perching [8]. The design of manipulators for aerial platforms often presents significant challenges, including constraints related to mass, volume, and the interaction dynamics between the arm and the flying platform. The limited payload capability of Mars Helicopter and volume constraints of the launch vehicle makes these constraints even more extreme.

All key and driving design constraints and requirements of SRH manipulation system are listed in detail in Section II. The Manipulation system design details are discussed in Section III, followed by control system overview in Section IV. Finally, some of the experimental results are reviewed in Section V.

## II. Design Requirements

SRH manipulation system is responsible for picking up the RGAs off an uneven terrain in the presence of rocks and dirt, stowing and retaining them during drive and flight to SRL while actuators are powered off, and dropping them off at the target zone. Before starting the design process, it was essential to clearly define design requirements based on how the system interacts with other subsystems and the environment around it, interfaces of the SRH to the manipulation system and SRL, and the terrain properties at the depot site. The key and driving requirements are introduced in this section.

### *A. Returnable Sample Tube and Glove Assembly (RGA)*

Perseverance rover carries a total of 43 RGAs, 10 of which are already filled up with samples and placed on the surface of Mars at Three Forks depot site. Made mainly of titanium, each RGA weighs 115g when empty and maximum 146g when filled up with samples (Figure 2). A white exterior coating guards against heating by the Sun that could potentially change the chemical composition of the samples after Perseverance deposits the RGAs on the surface of Mars. Manipulation system components shall avoid contacting the keep-out zone seal area at all times while handling an RGA.

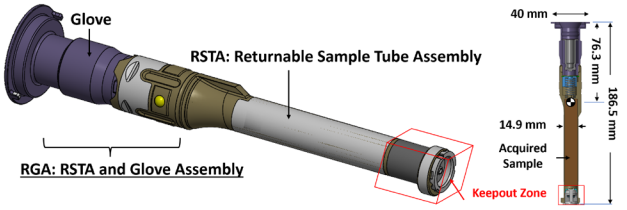


**Figure 2. Main parts and dimensions of RGA**

### *B. Mass and Volume*

The overall design of the SRH is significantly influenced by a strict mass limit due to the challenge of flying in the low-density Martian atmosphere. Manipulation was allocated an informal mass limit of 200 g, with the aim of reducing the mass as much as feasible. The SRH design faces another key challenge in fitting within specified volumes, namely the launch stow and operational stow not to exceed volumes (NTEs). These volumes are established in 3D and used throughout design process as guideline.

### *C. Payload Capability*

Considering all pertinent factors that influence available payload is crucial, as it directly impacts both structural and actuator design. The manipulation system's main task is to handle RGAs on Mars, namely picking up or dropping off empty or full RGAs (115g to 146g), with an additional 50g allowance for surface rocks. The system should also perform similarly on Earth while using a Mars-weighted RGA for testing. The varying sample amounts inside RGAs affect their mass properties, which are accounted for in the design.

### *D. Securing RGA for Transfer*

To avoid damaging the RGA or sample integrity during aerial and ground mobility operations, the manipulation system shall stow RGA securely on-board of the SRH. Additionally, the stow mechanism should limit the movement of the RGA relative to the SRH to keep the changes in the SRH mass properties within analyzed ranges and avoid impact loads and vibrations, which could detrimentally affect Aerial Mobility.

### *E. Grasp in Presence of Rocks*

Images and data provided by M2020 show that all 10 RGAs at the depot site in Three Forks are surrounded by pebbles and rocks ranging from sub-millimeter up to 30mm in greatest dimension (Figure 3). This can affect the functionality of the manipulation system, mainly the gripper, in two different ways.

#### *1) Rocks within Grasp*

Early exploratory testing and analysis revealed that the presence of surface rocks ranging from 0.5 – 20 mm in height or diameter significantly impacts RGA acquisition and potentially leads into grasp failure, loose or unstable RGA grasp, large misalignment in RGA with respect to the gripper after grasp, and uncertainty in grasp/stow confirmation. Since terrain around all RGAs is covered with rocks, and subsurface is likely to be similar, it is essential to ensure robustness to rocks of different sizes within given range.

#### *2) Ground Plane Compliance*

During RGA acquisition, the gripper fingers must stay below the centerline of the RGA to ensure a successful grasp. The terrain around RGAs in Three Forks has Z-height variability of ±20 mm and can be impervious due to the soil compactness and presence of embedded rocks. Moreover, the SRH pitch misalignment can further shift the fingers up or down in the Z direction. To eliminate the risk of gripper missing RGA, a terrain conforming feature, referred to as ground plane compliance, is required.

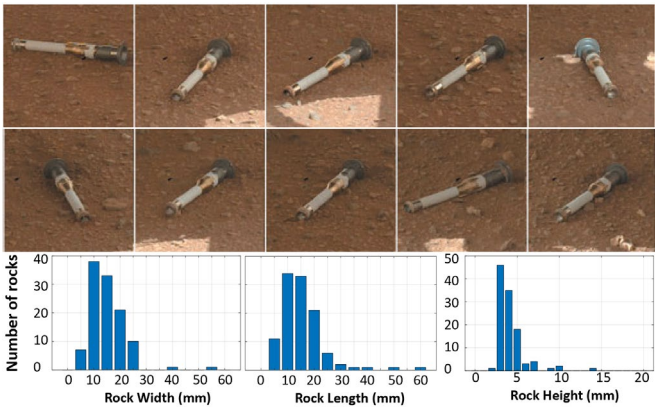


**Figure 3. Perseverance Rover data is used to analyze and extract size of the rocks around all 10 RGAs placed at the Three Forks**

## III. System Design

### A. Architecture Design

Given the constraints and requirements listed in Section II, an extensive trade study was conducted to determine the overall manipulation architecture. Eventually, the architecture shown in Figure 4 was found to best address the primary problems while meeting the constraints and optimizing for mass, system decoupling, and risk reduction. This designed architecture consists of a 3DOF planar robotic arm and a dual-actuator gripper with two sets of independently actuated compliant finger. The RGA was secured in the Gripper, while the Robotic Arm was stowed for flight via a constraining structure and spring-loaded detent at the wrist.

The architecture chosen embodies a true mobile manipulation platform. It divides control of different DOFs between the Ground Mobility and Manipulation elements to align the gripper with the terrain and RGA in all 6 DOFs, as illustrated in Figure 4. Ground Mobility actively controls the X, Y, and rotation about Z using its skid-steer system, while Manipulation controls the Y, Z, and rotation about X through a 3DOF planar Robotic Arm. Imperfect Ground Mobility positioning and terrain features in the vicinity of the RGA and SRH wheels leave residual misalignment in X, rotation about Y and rotation about Z. These misalignments are compensated through the implementation of the Gripper's compliant fingers and the finger grasp trajectories, ensuring all six DOF are effectively managed within the system.

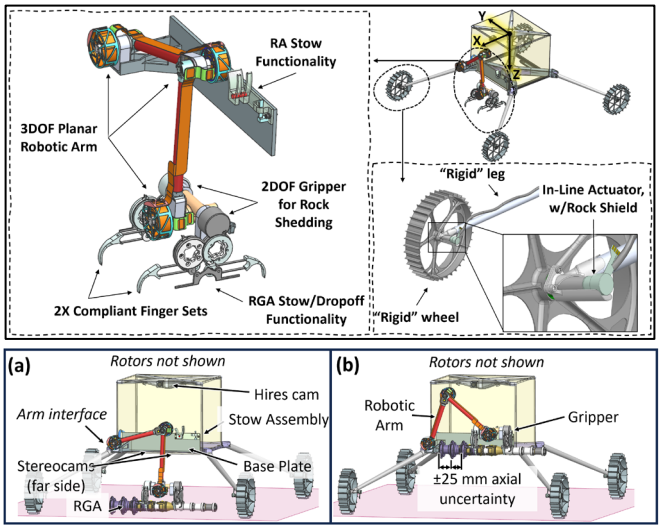


**Figure 4. SRH Architecture Design and Manipulation System (a) stowed (b) deployed**

### B. Robotic Arm Design

Key RA design factors are presented here, including workspace, kinematic parameters, torque requirements, and actuator design. Additionally, other important aspects were considered in design, including harness management, stow characteristics in presence of the dynamics of the host vehicle, structural design, and the interface with the SRH chassis.

#### 1) Workspace Definition

Defining the workspace properly is crucial for optimal sizing of the manipulation system elements. To this end, the SRH manipulation workspace is divided into three segments: surface, stow, and free-space workspaces. RGA Pickup is performed in the Surface Workspace, defined based on the RGA pose with respect to the RA base after the final drive. The integrated Ground Mobility positioning performance only drives the Y dimension of the Surface Workspace, as X, rotation about X, and heading angle errors drive the required gripper misalignment capability. This performance was empirically shown to achieve an accuracy of equal to or better than ± 15 mm along X, ± 40 mm along Y, and ± 5 deg heading (yaw) between RGA-fixed Grasp Frame and robot-fixed Arm Workspace Frame [9].

Once Ground Mobility is complete, terrain features like rocks, divots, and bumps cause pose variations between the RGA-fixed Grasp Frame and robot-fixed Arm Workspace Frame. These variations were analyzed relative to the average surface around each RGA using Perseverance Rover data to estimate height and tilt differences for the RGA and SRH chassis. This compiled information was then used to appropriately size the surface workspace (Figure 5).

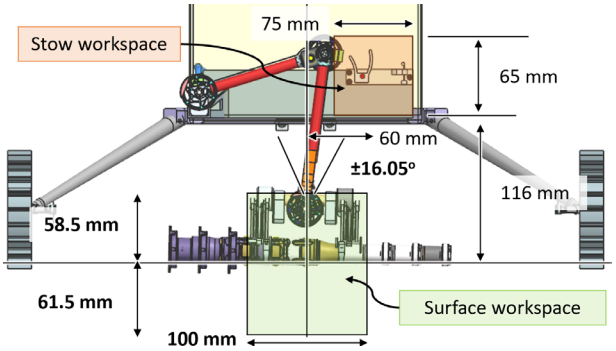


**Figure 5. Position and dimensions of the surface and stow workspaces. Robotic arm is depicted in Pickup pose where gripper is ready for grasp.**

A stow workspace is defined to ensure the arm and gripper can move to stow position and perform the necessary stow maneuver with or without RGA. The stowed position shall not interfere with rotor blades nor occlude any of the sensors or camera FOVs. The RGA can be in any clocked orientation within the grip, and ±25 mm along its axis (Figure 4), with RGA glove side always closer to the shoulder joint to reduce the torque on the RA joints.

Finally, a Free-Space workspace is defined to allow RA motion with the gripper between the Stow and Surface Workspaces. Definition of the Free-Space workspace also considers the RA positioning accuracy to ensure reachability to RGA offset poses that are guaranteed to be collision-free.

#### 2) Kinematic parameters

The first step in laying out the arm design was to find an initial kinematic configuration for the links based on the workspace definition. These kinematic parameters, depicted in Figure 6, are driven by reaching the -Y/+Z corner of the workspace, while also "minimizing" relative angles between links to both reduce actuator cycle count and avoid singularity at the edges of workspace. While numerous RA configurations can be derived for the Freespace workspace alone, the specific stow configuration results in the shoulder position located towards the lower +Y corner of the front face of the SRH body. The selected kinematic parameters were confirmed to fit within the designated volumes, as specified by the NTE volume requirements, using CAD models.

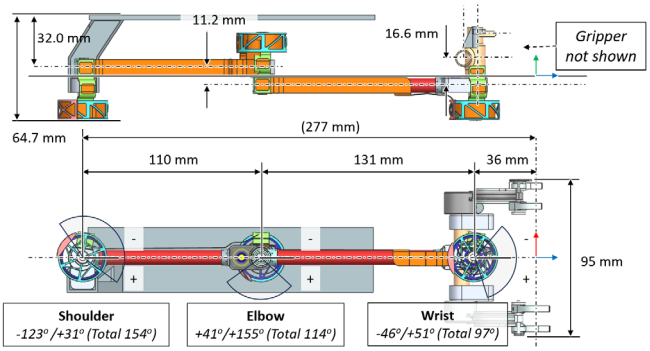


**Figure 6. Kinematic parameters of the Robotic Arm**

*3) Torque requirements*

To estimate the required joint torques, the RA's full motion path for unstow, pickup, and stow with RGA was simulated using RADAR (MATLAB based Robotic Assembly Design and Analysis Repository), a JPL internally developed MATLAB based tool [10]. Once a motion path with no collisions was found, RADAR was able to compute the expected joint torques for the operation. Figure 7 shows the results of the study.

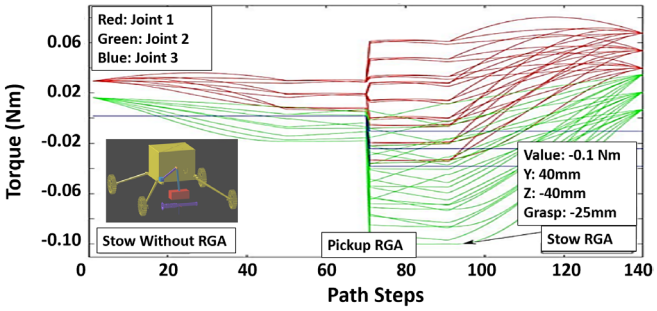


**Figure 7. Simulated motion under various pickup offset conditions and workspace locations in Mars gravity.**

Additionally, stow loads and contact loads of the RGA and Gripper were added to simulate those interactions. Resulting worst-case joint torques for these major operations are listed in Table 1.

**Table 1. Major operations worst-case loads in Mars and Earth gravity**

| Load | Contact Loads[1] [mNm] | | Un/Stow Loads[2] [mNm] | | Worst-case RGA[3] Lift Loads [mNm] | |
|---|---|---|---|---|---|---|
| Gravity | Mars | Earth | Mars | Earth | Mars | Earth |
| Joint 1 | 358 | 372 | 1069 | 1143 | 98 | 185 |
| Joint 2 | 261 | 262 | 1093 | 1137 | 110 | 158 |
| Joint 3 | 111 | 111 | 573 | 568 | 37 | 32 |

[1] Reporting worst-case of (2N, ±2N) in X-Y Planar loads
[2] The stow mechanism was assumed to produce the worst-case permutation of (±10N, ±10N) in X-Y Planar loads
[3] The RGA is Mars-weight mass analogue in earth gravity case

*4) Actuators*

To minimize the contractual costs of actuator development, it was deemed advantageous to align the actuator design across Ground Mobility, RA, and Gripper systems, thereby reducing skew and ensuring greater uniformity. This resulted in two actuator configurations. A Maxon brushless 8mm diameter motor, in combination with a 2562:1 8mm diameter planetary gearbox, was used for ground mobility and RA shoulder and elbow joints (16 g mass estimate). The same gearbox in combination with a Maxon brushless 6mm diameter motor was used for the RA wrist and gripper joints (13 g mass estimate). Both configurations use a preloaded output bearing pair wrapped around the planetary gearbox housing to improve output load handling capability (Figure 8). All RA and gripper joints are intended to be equipped with an absolute encoder with 0.088 deg resolution and 0.5 deg absolute accuracy.

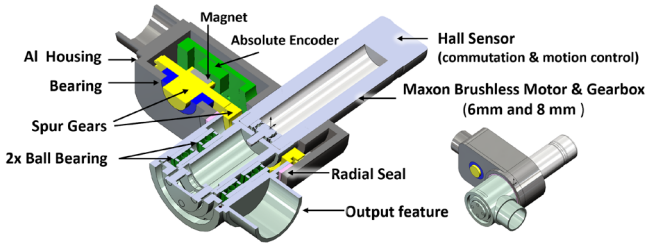


**Figure 8. RA and Gripper Actuator Design**

Another pivotal aspect of the design pertains to the actuator's back-drive capability. Considering the substantial number of stages in the planetary gearbox, it is presumed that the actuators will be non-back-drivable for short duration quasistatic loads (up to 6 Nm on gearmotor output). Initial testing conducted at Maxon company supports this hypothesis. However, for quasistatic sustained loads (up to 0.12 Nm on gearmotor output), the actuator can creep slowly in the driven direction. Thus, only aerial and ground mobility operations in which low sustained loads can be present introduce a risk of back-drive. It is noted that any creep at the output is detectable by the absolute encoders.

*5) Stowed Robotic Arm Characteristics*

The RA stowed configuration has a set of driving requirements that protect both the RA and the rest of the SRH during launch and operation. Initial actuator testing results showed the torsional stiffness of the actuators are notably low, at 13.64 Nm/rad. Consequently, to satisfy the minimum stowed frequency requirement, the stow mechanism must effectively restrict the torsional stiffness of each of the three RA actuators for launch and operation. This necessitates the implementation of a torsional lockout method. Furthermore, minimizing the offset of the center of gravity (CG) and the inertia of the gripper relative to the wrist would reduce the required torsional preload from the stow mechanism, and thus the RA torque to actuate it. This approach prevents both back-drive and oscillation at frequencies lower than 50 Hz.

*6) Structural Design*

The primary goal of design was to minimize mass, employing standard stress analysis techniques for metals and making certain assumptions for carbon fiber due to limited data availability. This entails employing typical analysis methods, including hand calculations incorporating JPL factor of safety and basic Finite Element Method (FEM) simulations to evaluate results. Attention is paid to factors such as stiffness and deflection to ensure optimal performance of the arm under operational conditions. RA links are made of carbon fiber tubes connected to the actuator output on one end and to the encoder box at the actuator input on the other end. Joint hard stops are also designed into the connectors. The gripper-wrist structure connects each half of gripper mechanism to the wrist joint output and includes the features to interface with the stow mechanism.

*7) Interface to SRH*

The manipulation system is mounted on a base plate that connects both the shoulder actuator (encoder) housing and the stow assembly to SRH leg structure (Figure 15). There are bolted interfaces between the stow assembly and manipulator base plate, and between the base plate and SRH. This separable assembly allows later integration to SRH, while being able to bench test entire manipulator and stow separately. This also allows stow assembly to be relatively well aligned with RA, as they are both attached to the same part.

## C. Stow Mechanism Design

The stow mechanism is designed to be activated and released by RA motion, eliminating the need for a separate actuator. To minimize mass and volume, the same RA stow method is used for both operational and launch stow without any additional launch lock devices. The stow sequence and related hardware are specifically designed to allow use of simple single-joint motions into and out of the stow position, avoiding compounding effects from kinematic calibration errors and differences in gravity between ground test and Mars surface operations. For RA stow, the arm itself provides the actuation to engage load shunt features mounted on the wrist output and a saddle and spring-loaded detent on the chassis stow assembly (Figure 9). As most of the mass of the Manipulation element is located at the wrist, this configuration reduced loads and increased the modal frequencies.

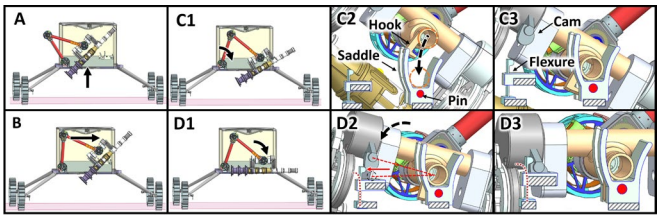


**Figure 9. Arm sequence of motion to stow with gripped RGA and details, as viewed from section at front face of SRH looking in +X. (C) elbow motion: hook and structure centered in Saddle, (D) wrist motion: cam deflects flexure and ends with preloaded wrist as the center hook rotates under the pin.**

*1) Stow Maneuver*

The projected length of the RGA is defined as the RGA length plus the 50 mm total axial uncertainty. Given that this length is greater than the projected distance between the landing gear struts at the gripper, the motion into stow must include some tilting motion. This motion also allows the RGA to be raised above the FOV of the stereocams and avoid contact with rotors. The last motion into stow and the first motion out of stow are performed by the wrist, after the wrist output has been partially seated in the stow assembly, which minimizes misalignment at the cam.

*2) Mechanical Implementation*

As depicted in Figure 9, the stow mechanism features an upward-facing (-Z) saddle with lead-ins in both YZ (joint sweep) and X directions (joint deflection), a pin to interface with the hook on the gripper-wrist structure, a flexure detent for torsional preload, a cam follower surface on the flexure detent to interface with the cam on the gripper-wrist structure, and a rectangular socket to constrain the cam, which also serves as the wrist rotational hardstop surface.

*3) Stow/unstow torque*

The stow mechanism was devised to utilize a torsional detent, actuated by the wrist joint and corresponding features on the wrist-gripper structure. By ensuring the gripper CG is approximately located at the wrist, the torsional requirement is based on moment of inertia. However, while holding the RGA at an offset from the wrist, the required torque to resist inertia was approximated to be well within the wrist actuator capability. An asymmetric cam profile is used to only see this torque when moving to release the RA from the detent to minimize high torque cycles on the actuator.

## D. Gripper Design

During the initial phase of the gripper design, several technologies were evaluated, including bi-stable devices, passive mechanisms, granular jamming systems, and phase-changing materials. Subsequently, the design space was narrowed down to solely incorporate the classic approach of utilizing a drive mechanism to manipulate mechanical fingers for grasping and picking up RGAs. This decision was primarily based on the technology readiness level (TRL) and programmatic consideration within the SRH project.

*1) Gripper Capability*

The gripper shall be able to grip an RGA in the presence of up to ± 15 mm misalignment about X and up to ± 5 deg heading (yaw) error simultaneously, resulting from Ground Mobility final drive. Additionally, any pitch angle (rotation about Y) misalignment between gripper base frame and RGA shall be compensated by the gripper capability.

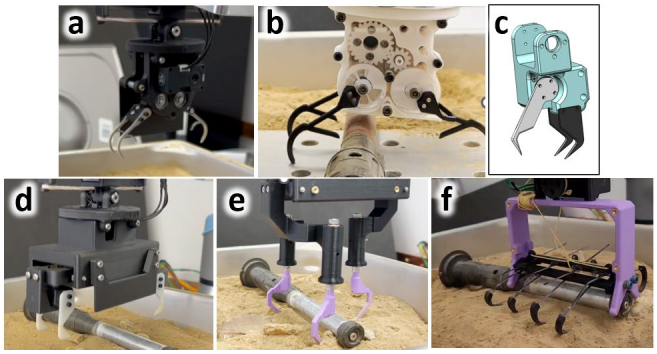


**Figure 10. Exploratory gripper testing (a) classic gripper (fingers on revolute joints) w/ 2DOF Wrist, (b) classic gripper with compliant fingers, (c) mini-rake (d) prismatic drive w/ 2DOF Wrist, (e) prismatic drive w/ prismatic fingers, (f) Clamshell**

*2) Exploratory Test Campaign*

To gain a better understanding of how the design requirements can affect gripper design, a number of design candidates were prototyped and tested using a UR3 robotic arm under various conditions, including rock size, rock placement, and misalignment between gripper and RGA. More specifically, the addition of compliance at the wrist vs. directly at fingers, the number and spacing of the fingers, and the type of drive mechanism were parameters of interest that were explored in the prototyped units. The resulting design candidates are depicted in Figure 10, and below is a summary of the test campaign result. These results were then used to inform the final gripper design, as explained in the remaining part of this section.

- Moving gripper to contact RGA or terrain prior to attempting grasp leads to higher grasp success rate.
- Fingertip motion which stays below lower half of RGA leads to high rate of grasp success; ideally, this motion sweeps across ground, followed by an upward motion.
- It's very likely that rocks and regolith are captured between fingers and RGA, which can lead to significant misalignment and instability between gripper and RGA, depending on the gripper design.
- RGA isn't likely to remain "stuck" in terrain, but glove flange will act as temporary anchor/pivot point until a moment is applied.

*3) Rock Shedding*

The test campaign results proved that the rocks and pebbles around RGA are likely to be inadvertently picked up alongside the RGA, necessitating the incorporation of a function within the gripper to dislodge such debris once the grasp is completed. An alternating grip system was designed to address this and shed rocks prior to flying back towards SRL. This consists of two separately actuated set of fingers that go through a sequence of opening and closing to drop off any rocks captured during pick up. An alternate approach was considered that used a separate RGA stow mechanism to allow rocks to fall off during the hand off of RGA from the gripper. However, analysis revealed that a successful hand-off would require this solution to precisely position the RGA within the stow system, including accommodation of RGA misalignment induced by the captured rocks, as well as to manage and solve complex load cases, both of which proved challenging within the given volume and mass constraints.

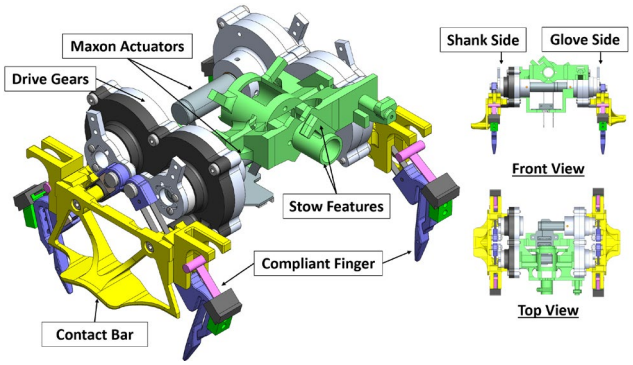


**Figure 11. Gripper assembly is composed of two separately actuated subassemblies. The stow features are designed into the gripper structure that connects the two subassemblies.**

Furthermore, a mass study indicated that utilizing the alternating grip system would result in a slightly lighter overall configuration. An additional inherent benefit of the alternating grip approach is increased width of grasp and consistent positioning of the RGA center of gravity between the fingers. This configuration effectively prevents cantilevered moment loads on the gripper fingers from the RGA, thereby significantly improving the grasp quality and overall stability of the system.

*4) Drive mechanism*

A linkage-based mechanism is designed to generate a predefined path of motion, ensuring the tips of the fingers sweep across the surface horizontally. A geometric design approach using three point of accuracy was used to size the length of the mechanism links. At the end of the grasp motion, the mechanism reaches an over-center configuration (Figure 12), enabling a non-back-drivable grip with loads applied at the fingers. Furthermore, the compliant length of the fingers is effectively reduced, approaching to zero at the motion conclusion, making the grasp almost rigid and complying with vibration requirement of the system. This design not only ensures a precise motion but also yields a strong and non-back-drivable grip, making it a robust solution for grasp anywhere along the axis of the RGA. The drive mechanism can open the fingers to handle up to ± 25 mm of X misalignment in RGA position, large enough to handle simultaneous residual X and heading angle misalignment from Ground Mobility.

*5) Finger compliance*

The uneven surface at the pickup site, exacerbated by the presence of rocks, demands the gripper fingers to comply with this irregularity at the time of initial contact, during the contact detection process, and throughout the sweeping motion leading to grasp. The compliance not only enhances the gripper's ability to adapt to surface irregularities but also serves to prevent fingers from becoming ensnared behind anchored rocks, thereby ensuring operational reliability and robustness.

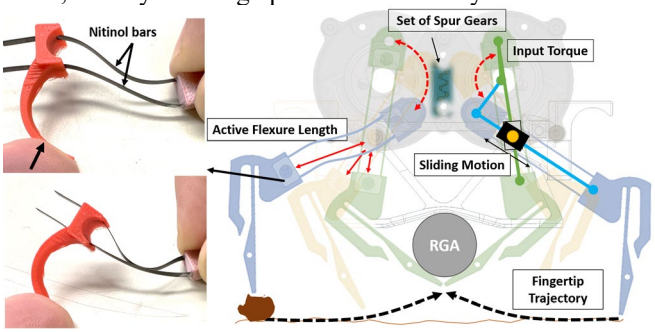


**Figure 12. A linkage-based mechanism generates the desired fingertip path of motion which concludes into an over-center position.**

The gripper test campaign indicated that implementation of compliance directly at the fingers can be more advantageous than incorporation of a compliant mechanism at the wrist; it is also believed that the design of a lockout mechanism for wrist compliance would be a comparatively more complex and heavier solution. The innovative design of the compliant fingers includes two parallel, flexible nitinol bars, offering a robust solution with several distinct benefits (Figure 12). By significantly stiffening the fingers in the out-of-plane direction, they effectively prevent twisting, ensuring stability during operation. Additionally, acting as a 4-bar linkage, this mechanism maintains the fingers consistently perpendicular to the surface. Finally, the mechanism also acts as a load limiter in which the top beam can buckle under higher loads if the finger were to catch on a rock in its path, creating a bi-modal anchored rock release mechanism, thus enhancing the gripper's overall performance. Nitinol is selected for its property of hyper-elasticity, should loads exceed expectations.

The compliance in the fingers is designed to have 20mm deflected vertical range of motion to conform to the tallest rocks at the pickup site. The deformation is designed to be achievable with a maximum normal contact force of 3N applied by the RA. The compliance of the fingers is continually reduced throughout the grasp motion, with the fingers becoming almost rigid as grasp is completed.

## IV. Software and Control

As a part of the larger SRH vehicle, the manipulation subsystem only interacts with a subset of the onboard sensors and actuators. At its core, Manipulation must control 5 independent motors, monitor the onboard Inertial Measurement Unit (IMU), and acquire images from a stereo pair to perform all necessary functions. Figure 13 shows the high-level interplay between hardware, electronics, and software distributed among the various onboard computers.

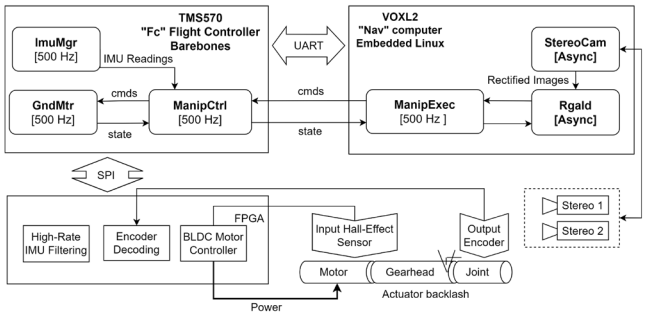


**Figure 13. Simplified diagram of mechanical, electrical, and software elements used by the Manipulation System**

### A. Computers

There are three types of onboard computers on SRH leveraged heavily from the Ingenuity tech demo avionics [11]. A ProASIC3 Field-Programmable Gate Array (FPGA) performs closed loop BLDC motor control, Position Encoder decoding, and high-rate sampling of the IMU. The reliable TI TMS570 ARM Cortex-R5 computer interfaces to the FPGA via SPI and performs self-contained functional autonomy behaviors needed for RA and gripper control, including fault handling. Finally, the Modal-AI VOXL2 is an embedded Linux computer that provides interface with the TMS570 over UART and runs the high-level control including Command and Data Handling (C&DH) for functions such as logging and sequencing, Camera drivers, RGA pose estimation, and executive behaviors to enable end-to-end RGA acquisition and drop-off.

### B. Sensing

The mass and dimensional constraints demand that SRH be designed with as few sensors and actuators as strictly necessary. A single RTD temperature sensor is bonded onto the first shoulder joint and used to seed a thermal model upon wake-up. A stereo camera pair is used by the pose estimator to estimate the pose of the RGA. Each actuator is equipped with a motor-side hall-effect sensor used for low-level motor control and a 12-bit output absolute encoder which serves multiple related functions. The output sensor monitors for position creep when the motor is unpowered during aerial and Ground Mobility, enables a backlash-compensating output position controller, and detects gripper contact with the RGA on the ground by crude torque estimation and/or by direct backlash crossing. Motor winding currents are estimated by sensing the voltage drop across a shunt resistor on the Motor Driver supply and dividing by the commanded duty cycle.

### C. Actuator Control

The GndMtr software component implements a PID controller to perform closed-loop motor control via SPI registers on the FPGA. Commutation is handled by a TI MCT8316Z BLDC Driver chip which accepts the motor-side hall sensor as direct input. Along with motor control, the GndMtr component implements a thermal fault model to prevent damage to the motor windings and relays the current monitor to downstream consumers.

The ManipCtrl software component offers various motion commands to control the RA and gripper. To accomplish single and multi-axis coordinated motion, it uses a linear segment with parabolic blends profiler. A classical backlash-aware outer loop position controller is used for output position control. Finally, it also monitors IMU for tip-over prevention and contact detection for reducing Z-height uncertainty. The control scheme is depicted in Figure 14.

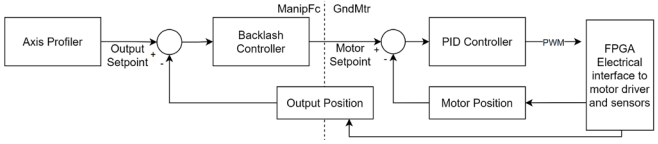


**Figure 14. Actuator Output Position Control**

### D. Contact Detection

Preliminary analysis indicates that estimating deflection torque across the geartrain and characterizing the other sources for parasitic torque losses may be sufficient to performing contact detection through online joint torque estimation. Using this approach, the net reaction torque is computed online for each joint, and when any joint deviates from the free-space expected joint torque by sufficient margin, contact with the environment is triggered. The major challenge is to register contact before a max load of approximately 5N is reached and risk of tip-over is deemed unacceptably high as we depend on the IMU for fault response and not as baseline contact detection.

## V. System Performance

### A. Prototype Fabrication

To evaluate performance of the SRH surface robotics systems, including both Ground Mobility and Manipulation, a complete prototype was fabricated. The prototype of the manipulation system and all its components are depicted in Figure 15.

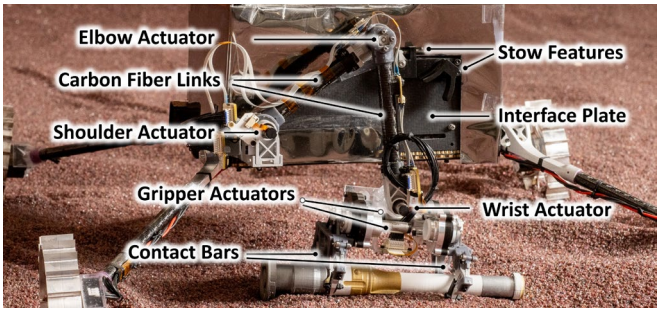


**Figure 15. Manipulation System prototype successfully grasping RGA.**

The three RA actuators and two gripper actuators are bonded to machined aluminum housings that provide appropriate interfaces to assemble the rest of the components. An aluminum bracket mounts the arm onto the interface plate, while the stow features are machined and bolted onto the same plate. The gripper fingers were prototyped using flexible nitinol bars, 4mm wide and 0.25mm thick, bonded to the rigid

aluminum portions of the fingers. A two-part epoxy resin was used for all bonding procedures. Wiring was completed using commercially available flat cables for this prototype.

### B. Test Runs

The test runs start with setting the SRH at an initial distance from the RGA based on aerial system landing accuracy estimate. The system then uses an onboard RGA identification algorithm to detect the position of the RGA and drives to it. Once the ground mobility is completed, the manipulation system starts RGA acquisition. A time-lapse of pickup sequence is depicted in Figure 16. So far, over 25 surface robotics test runs have been completed, in all of which the manipulation system has successfully picked up and stowed the arm and RGA.

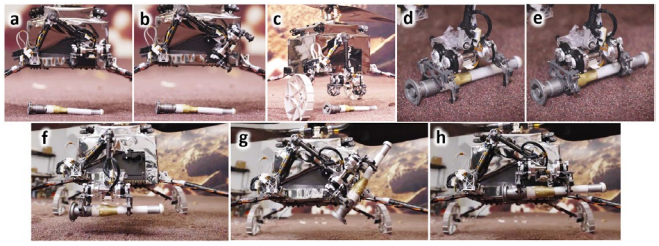


**Figure 16. Time-laps of RGA pickup test: (a) ground mobility complete (b) arm unstow (c) gripper at ready for pickup pose (d) gripper contact with RGA detected (e) gripper closes (f) ready for rock shedding (g) stow maneuver (h) stow complete and ready for drive/flight.**

## VI. Conclusion

In conclusion, this paper has presented the design, prototyping, and testing of a specialized lightweight robotic arm and gripper tailored for autonomous operation on Mars' uneven and rocky surface. Through the formulation and prototype testing of the SRH concept, the feasibility of RGA retrieval using combined aerial and ground mobile manipulation systems has been demonstrated. This effort underscores the potential for future mobile manipulation missions on planetary bodies, facilitated by small surface spacecraft, which offer cost-effective delivery and accommodation for hosted missions.

The advantages of small platform mobile manipulation are evident, with applications spanning instrument deployment, sample retrieval, and craft docking. The successful operation of the SRH concept and Ingenuity on Mars establishes a solid foundation for future surface exploration missions employing small robotic spacecraft. Notably, the SRH manipulation system is unique compared to recently formulated and flown space manipulation systems due to its effective use of passive compliance in the gripper for engaging with uncertain and unstructured targets. We expect that the growth in complexity of space-based manipulation tasks and further engagement with space surface environments in upcoming lunar missions will find increased use for robotic manipulation mechanisms similar to the SRH gripper.

## Acknowledgment

Thanks to NASA, AeroVironment, NASA Ames Research Center, and the entire M2020 Perseverance Team for supporting the development of SRH. The decision to implement Mars Sample Return will not be finalized until NASA's completion of the National Environmental Policy Act (NEPA) process. This document is being made available for information purposes only. The research was carried out at the Jet Propulsion Laboratory, California Institute of Technology, under a contract with the National Aeronautics and Space Administration (80NM0018D0004).

## VII. References

[1] F. Mier-Hicks, H. F. Grip, A. Kalantari, S. Moreland, B. Pipenberg, M. Keennon, T. K. Canham, M. Pauken, E. Decrossas, T. Tzanetos and J. B. Balaram, "Sample Recovery Helicopter," in *2023 IEEE Aerospace Conference*, 2023.

[2] J. Papon, R. Detry, P. Vieira, S. Brooks, T. Srinivasan, A. Peterson and E. Kulczycki, "Martian Fetch: Finding and retrieving sample-tubes on the surface of mars," in *2017 IEEE Aerospace Conference*, 2017.

[3] A. Kalantari and M. Spenko, "Modeling and Performance Assessment of the HyTAQ, a Hybrid Terrestrial/Aerial Quadrotor," *IEEE Transactions on Robotics,* vol. 30, pp. 1278-1285, 2014.

[4] E. Sihite, A. Kalantari, R. Nemovi, A. Ramezani and M. Gharib, "Multi-Modal Mobility Morphobot (M4) with appendage repurposing for locomotion plasticity enhancement," *Nature Communications,* vol. 14, p. 3323, 2023.

[5] C. S. K. H. Kim S, "Aerial manipulation using a quadrotor with a two dof robotic arm," in *IEEE/RSJ international conference on intelligent robots and systems*, Tokyo, Japan, 2013.

[6] H.-N. Nguyen, C. Ha and D. Lee, "Mechanics, control and internal dynamics of quadrotor tool operation," *Automatica,* vol. 61, pp. 289-301, 2015.

[7] M. T. Pope, C. W. Kimes, H. Jiang, E. W. Hawkes, M. A. Estrada, C. F. Kerst, W. R. T. Roderick, A. K. Han, D. L. Christensen and M. R. Cutkosky, "A Multimodal Robot for Perching and Climbing on Vertical Outdoor Surfaces," *IEEE Transactions on Robotics,* vol. 33, pp. 38-48, 2017.

[8] P. Spieler, S. X. Wei, M. Li, A. Galassi, K. Uckert, A. Kalantari and J. W. Burdick, "PARSEC: An Aerial Platform for Autonomous Deployment of Self-Anchoring Payloads on Natural Vertical Surfaces," in *2023 IEEE International Conference on Robotics and Automation (ICRA)*, 2023.

[9] W. Reid, A. Bouton, M. P. Strub, M. Newby, S. Gerdts, J. Martin, S. Moreland and R. McCormick, "Planning and Control for Autonomous Drives of the Mars SampleRecovery Helicopter," in *2024 IEEE Aerospace Conference*, 2024.

[10] J. Jenkins, M. Dolci, C. Collins and P. Younse, "Robotic Arm Design and Analysis Repository (RADAR)," in *2022 IEEE Aerospace Conference (AERO)*, 2022.

[11] B. Balaram, T. Canham, C. Duncan, H. F. Grip, W. Johnson, J. Maki, A. Quon, R. Stern and D. Zhu, "Mars Helicopter Technology Demonstrator," in *2018 AIAA Atmospheric Flight Mechanics Conference*.